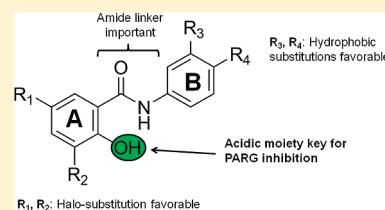


Discovery and Structure–Activity Relationships of Modified Salicylanilides as Cell Permeable Inhibitors of Poly(ADP-ribose) Glycohydrolase (PARG)

Jamin D. Steffen,[†] Donna L. Coyle,[†] Komath Damodaran,[‡] Paul Beroza,^{‡,§} and Myron K. Jacobson^{*,†}[†]Department of Pharmacology and Toxicology, College of Pharmacy and Arizona Cancer Center, University of Arizona, Tucson, Arizona 85724, United States[‡]Telik, Inc., 700 Hansen Way, Palo Alto, California 94304, United States

ABSTRACT: The metabolism of poly(ADP-ribose) (PAR) in response to DNA strand breaks, which involves the concerted activities of poly(ADP-ribose) polymerases (PARPs) and poly(ADP-ribose) glycohydrolase (PARG), modulates cell recovery or cell death depending upon the level of DNA damage. While PARP inhibitors show high promise in clinical trials because of their low toxicity and selectivity for BRCA related cancers, evaluation of the therapeutic potential of PARG is limited by the lack of well-validated cell permeable inhibitors. In this study, target-related affinity profiling (TRAP), an alternative to high-throughput screening, was used to identify a number of druglike compounds from several chemical classes that demonstrated PARG inhibition in the low-micromolar range. A number of analogues of one of the most active chemotypes were synthesized to explore the structure–activity relationship (SAR) for that series. This led to the discovery of a putative pharmacophore for PARG inhibition that contains a modified salicylanilide structure. Interestingly, these compounds also inhibit PARP-1, indicating strong homology in the active sites of PARG and PARP-1 and raising a new challenge for development of PARG specific inhibitors. The cellular activity of a lead inhibitor was demonstrated by the inhibition of both PARP and PARG activity in squamous cell carcinoma cells, although preferential inhibition of PARG relative to PARP was observed. The ability of inhibitors to modulate PAR metabolism via simultaneous effects on PARPs and PARG may represent a new approach for therapeutic development.



INTRODUCTION

Activation of poly(ADP-ribose) (PAR) metabolism is an immediate response to genotoxic stress that promotes cell recovery at low levels of damage and cell death at high levels.^{1,2} In response to DNA strand breaks, PAR synthesis is catalyzed from NAD⁺ by poly(ADP-ribose) polymerases 1 and 2 (PARP-1/2) and PAR degradation is catalyzed by poly(ADP-ribose) glycohydrolase (PARG).^{3–5} Activation of PARPs-1/2 results in the rapid accumulation of large, multibranched PAR⁶ that covalently modifies PARP-1, histones, p53, and nuclear proteins involved in DNA repair.⁷ At higher levels of DNA damage, the coordinate activities of PARPs-1/2 and PARG can rapidly deplete the pool of cellular NAD(H), facilitating the release of mitochondrial proteins through signaling pathways that promote cell death.^{8,9}

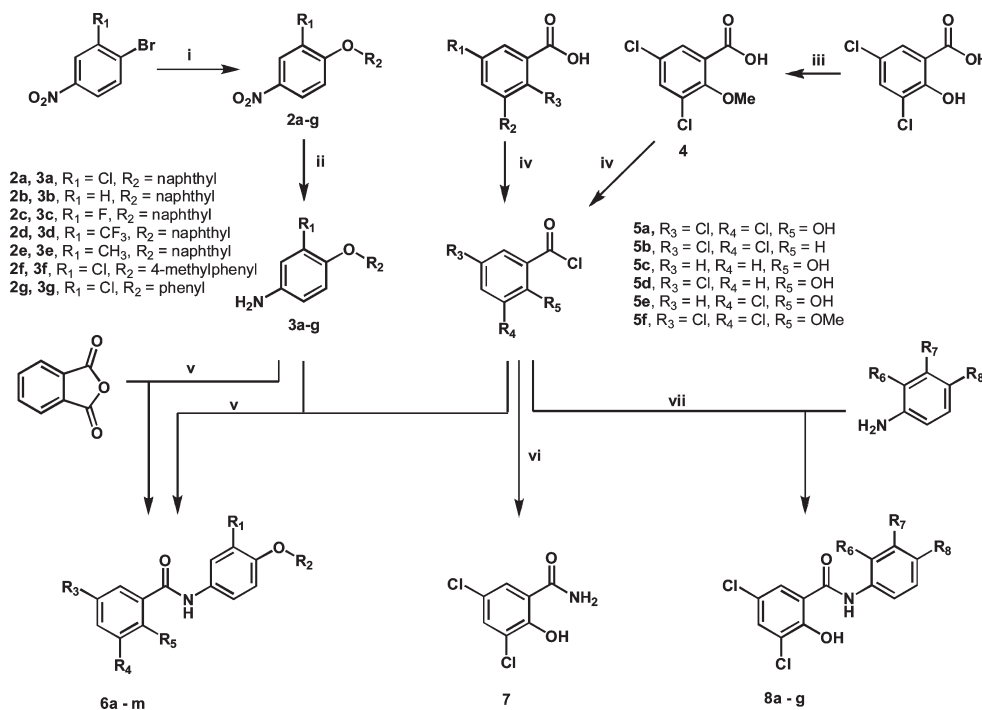
Enzymes involved in PAR synthesis are promising therapeutic targets with development focused on PARP-1, the main synthesizing enzyme of PAR with a well-defined role in cell fate determination,^{10–12} although PARP-2 selective inhibitors have been reported.¹³ PARP inhibitors are very well tolerated and have shown much promise in late stage clinical trials adjunctive with chemotherapy for triple negative breast cancers and as monotherapy for BRCA1/2 cancers.^{14–16} Much less is known concerning the therapeutic potential of PARG.¹⁷ The lack of high-throughput screening methods, lack of a crystal structure,

and lack of bioavailable inhibitors have limited the evaluation of PARG. Complete PARG knockouts in mice are embryonic lethal,¹⁸ but deletion of the nuclear isoform of PARG results in hypersensitivity to DNA alkylating agents and radiation, demonstrating the requirement of a close coordination between PARP and PARG activities for responses to DNA damage.^{19,20} RNA interference approaches have aimed to overcome some of the limitations associated with the gene manipulation but have been limited by the inability to completely suppress PARG activity.^{21–23} However, PARG knockdown in combination with disruption of base excision repair has been shown to enhance the cytotoxicity of temozolomide.²⁴ There are several reports of PARG inhibitors consisting of hydrolyzable tannins,^{25–27} ethacridine,²⁸ the ADP-ribose analogue ADP-(hydroxymethyl)pyrrolidinediol (ADP-HPD),^{29–31} and *N*-bis-(3-phenylpropyl)-9-oxofluorene-2,7-diamide (GPI 16552).³² While these inhibitors have shown utility in vitro, questions pertaining to potency, selectivity, and cell permeability remain.^{33–35}

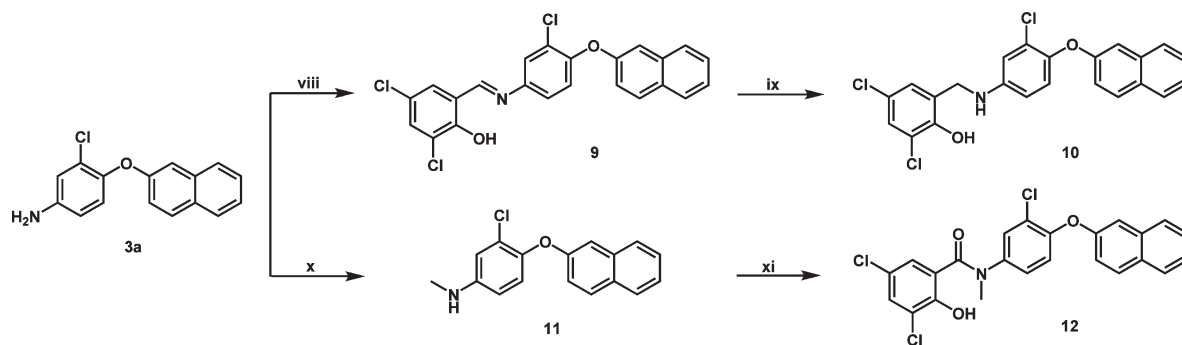
As an alternative to a high-throughput screening, we applied target-related affinity profiling (TRAP) to identify the initial PARG inhibitors described in this report.³⁶ TRAP technology characterizes a chemical library of small molecules by their binding

Received: March 21, 2011

Published: June 21, 2011

Scheme 1. Synthesis of A-Ring, B-Ring, and C-Ring Substituted Analogues^a

^a Reagents and conditions: (i) HO-R, Cs₂CO₃, 90 °C, 24 h; (ii) SnCl₂, EtOH, 70 °C, 3 h; (iii) CH₃I, acetone, K₂CO₃, reflux, 3 h; (iv) SOCl₂, 100 °C, 30 min; (v) CH₂Cl₂, room temp; (vi) NH₄OH, CH₂Cl₂, room temp; (vii) H₂N-R, ether, room temp.

Scheme 2. Synthesis of Linker Modified Analogues^a

^a Reagents and conditions: (viii) 3,5-dichlorosalicylaldehyde, EtOH; (ix) NaCNBH₃, EtOH; (x) CH₃I, acetone, K₂CO₃, reflux 3 h; (xi) 5a, CH₂Cl₂, room temp.

affinities to a panel of proteins, which defines an “affinity fingerprint”. Activity information for a set of compounds (e.g., IC₅₀) is combined with the affinity fingerprints of the compound to construct a fingerprint-based model for bioactivity. This model is used to select additional compounds for testing. Screening proceeds in an iterative manner, with batches of ~70 compounds tested followed by computational model refinement at each iteration. Such iterative cycles of compound selection, experimental assay, and model refinement have shown success in identifying bioactive molecules across a number of therapeutic targets.³⁶

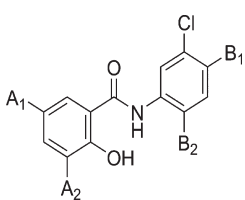
CHEMISTRY

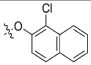
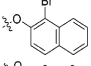
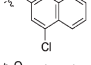
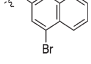
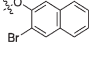
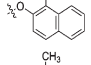
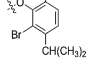
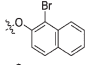
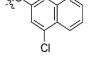
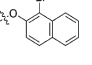
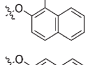
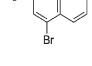
The simplest route to obtain salicylanilides involves amide coupling between commercially available salicylic acids and

anilines (Scheme 1). The substituted amines 3a–g were created by cross-coupling selected nitrobenzenes with various phenols using Cs₂CO₃ as the base in excess (3 equiv) at 90 °C, to obtain the substituted nitrobenzenes 2a–g. These nitrated compounds were selectively reduced to amines 3a–g in the presence of excess stannous chloride (SnCl₂) in ethanol. Benzoic acids were converted to acid chlorides 5a–f by addition of excess thionyl chloride (SOCl₂) under reflux. Hydroxyl methylation of 3,5-dichlorosalicylic acid was carried out prior to thionyl chloride treatment, by refluxing with potassium carbonate and iodomethane in acetone to give 4. The acid chlorides were coupled to corresponding amines in CH₂Cl₂ to generate 6a–m, 7, 8a–g.

The Schiff base 9 was readily formed by the mixture of 3,5-dichlorosalicylaldehyde and substituted amine 3a in ethanol

Table 1. Active Salicylanilides Identified from TRAP Screening

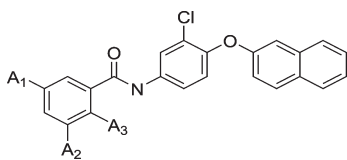


Cmpd	A1	A2	B1	B2
1a	Cl	Cl	H	
1b	Cl	Cl	H	
1c	Cl	Cl	H	
1d	Cl	Cl	H	
1e	Cl	Cl		H
1f	Cl	Br	H	
1g	Cl	Br	H	
1h	Cl	I	H	
1i	Cl	I	H	
1j	Cl	H		H
1k	Br	Br	H	
1l	Br	Br	H	

(Scheme 2). When this product was reacted with an excess of sodium cyanoborohydride (5 equiv) in ethanol, the Schiff base was selectively reduced to the amine **10**. Mono-*N*-alkylation of **3a** was achieved by refluxing the amine and potassium carbonate in acetone in the presence of iodomethane (5 equiv). This reaction gave both the mono-*N*-methyl **11** and di-*N*-methyl products, which were separated by column chromatography. Compound **11** was coupled to **5a** in CH_2Cl_2 to generate **12**.

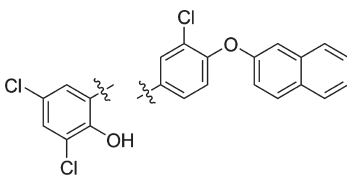
RESULTS AND DISCUSSION

A Novel Screening Approach Has Led to the Discovery of Lead PARG Inhibitors. Target-related affinity profiling (TRAP)³⁶ was used to search for lead inhibitors of PARG. For each round of screening, a hit was defined as a compound showing 70% inhibition of PARG at a defined concentration of test compound. In most cases, hits were subjected to dose-response evaluation to establish an approximate IC_{50} . Four iterations of screening were completed, and ~70 compounds were tested in each round. In total, 296 compounds were

Table 2. SAR of A-Ring Substituted Analogues^a


compd	A ₁	A ₂	A ₃	PARG IC_{50} (μM)
6a	Cl	Cl	OH	12 ± 2
6b	Cl	Cl	H	NI
6c	H	H	OH	~500
6d	Cl	H	OH	117 ± 60
6e	H	Cl	OH	61 ± 12
6f	Cl	Cl	OMe	NI
6g	H	H	COOH	72 ± 7

^a NI (noninhibitory): no detectable inhibition of PARG up to 500 μM .

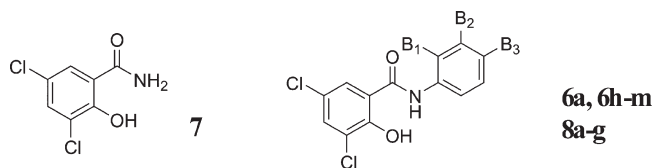
Table 3. SAR of Linker Modified Analogues^a


Cmpd	PARG IC_{50} (μM)
5a	12 ± 2
9	NI
10	NI
12	140 ± 20

^a NI (noninhibitory): no detectable inhibition of PARG up to 500 μM .

evaluated and ~30 compounds were identified with IC_{50} values below 100 μM . Of these, the 24 best hits were screened a second time at 10 μM and the 12 compounds with the highest degree of inhibition at this concentration were selected as the lead hits. The chemotype of the vast majority of these compounds was a substituted salicylanilide motif (Table 1). Common substitutions included the presence of a halide at two positions on the A ring of the salicylanilide (labeled A1 and A2) in 11 of the 12 hits, a chloro substitution on the B ring, and an aromatic moiety attached to the B ring.

SAR Studies Have Defined a New Pharmacophore for PARG Inhibition. To further explore the SAR relationships for PARG inhibition, we synthesized a series of additional salicylanilide analogues. Compound **1e** was taken forward as the lead hit, since it contained the greatest selectivity toward PARG over PARP-1. Initially **1e** was modified by removal of the C-ring bromo-substitution **6a** to remove a significant amount of molecular weight without losing significant activity. To determine

Table 4. SAR of B-Ring and C-Ring Substituted Analogues^a

Cmpd	B1	B2	B3	PARG IC50 (μM)
6a	H	Cl		12 ± 2
6h	H	H		42 ± 9
6i	H	F		27 ± 2
6j	H	CF ₃		21 ± 3
6k	H	CH ₃		25 ± 7
6l	H	Cl		26 ± 2
6m	H	Cl		61 ± 10
7	-	-	-	NI
8a	H	Cl	OH	NI
8b	Cl	H	H	PI
8c	H	Cl	H	261 ± 75
8d	H	H	Cl	~500
8e	CH ₃	H	H	PI
8f	H	CH ₃	H	PI
8g	H	H	CH ₃	PI
8h	H	H	H	NI

^aNI (noninhibitory): inhibition of PARG does not exceed 10% at 500 μM. PI (partially inhibitory): inhibition of PARG is between 10% and 30% at 500 μM.

the importance of the A ring hydroxyl and halo substitutions, a number of analogues were synthesized and tested for PARG inhibition (Table 2). Removal of the hydroxyl group at position A3 **6b** resulted in loss of detectable inhibition of PARG, establishing this group as an important feature of the pharmacophore. Removal of both chloro substitutions **6c** resulted in more than a 50-fold decrease in potency, while removal of single chloro substitution **6d**, **6e** decreased potency 5- to 10-fold. The requirement of a chloro substitution for inhibition led us to hypothesize that an acidic hydroxyl was a component of the pharmacophore rather than a hydrogen bond donor (HBD) hydroxyl. This hypothesis was supported by the observation that methylation of the hydroxyl group **6f** resulted in the loss of detectable PARG inhibition. In addition, PARG inhibition was retained when the acidic hydroxyl was replaced with a carboxylic acid **6g**. In total, these experiments demonstrate an acidic substitution at the position of the A ring hydroxyl as a key component of the PARG inhibition pharmacophore.

The next approach in defining the pharmacophore involved characterizing the involvement of the amide linker in PARG inhibition. Toward this end, a number of analogues were synthesized and tested for PARG inhibition properties (Table 3). The absence of the carbonyl group and amide hydrogen **9** resulted in loss of PARG inhibition. Removal of just the carbonyl group **10**

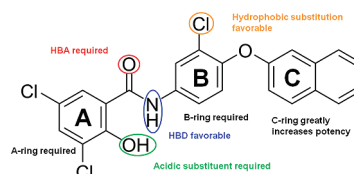


Figure 1. Key pharmacophoric elements related to PARG inhibition.

also resulted in a loss of PARG inhibition. Methylation of the amide nitrogen **12** resulted in a 10-fold loss of PARG inhibition. These results argue that the pharmacophore involves the presence of a hydrogen bond acceptor (HBA), while the HBD is dispensable but favorable for PARG inhibition.

SAR experiments also examined the involvement of the B ring and C ring in PARG inhibition. A number of analogues were prepared that eliminated or modified the B ring and/or C ring (Table 4). Complete elimination of the C-ring **8a** resulted in a complete loss of PARG inhibition. When the hydroxyl was removed from the B-ring **8c**, PARG inhibition returned although at low potency. It is likely the acidic nature of the hydroxyl on the B-ring in compound **8a** is very unfavorable. When the C-ring was deconstructed to a 4-methylphenyl **6l** and phenyl substitution **6m**, potency was decreased 2-fold and 5-fold, respectively. Collectively these compounds indicate that a large, hydrophobic substitution is favorable at the C-ring position.

Elimination of the C-ring and B-ring **7** resulted in loss of detectable PARG inhibition. Replacement of the B-ring in the absence of any B-ring substitution **8h** was still not enough to detect PARG inhibition. Only once the B-ring chloro-substitution **8c** was replaced, was PARG inhibition detected again. Displacement of the chloro-substitution to the ortho and para positions of the B-ring **8b**, **8d** resulted in a slight loss of potency. Switching out the chloro-substitution for a methyl substitution at all three positions **8e–g** on the B-ring also resulted in a slight loss of potency. This indicated that the B-ring substitution may serve to provide hydrophobicity rather than electron-withdrawing effects important for potency. To test this observation, substitutions were made at the B-ring in the presence of the C-ring. Replacing the chloro-substitution of the B-ring with substitutions of greater electronegativity **6i**, **6j** resulted in nearly a 2-fold loss in potency. When a methyl group was added instead **8k**, again only a slight loss of potency was observed. However, removal of a substitution at this position **8h** resulted in a 3-fold loss in potency. Taken together it is indicated that this B-ring substitution slightly contributes to PARG inhibition because of its hydrophobicity rather than electron-withdrawing effects. These experiments define the B-ring and B-ring substitution as a necessary component of the pharmacophore, but potency is greatly enhanced by the presence of the C-ring. Figure 1 represents the pharmacophore for PARG inhibition derived from the SAR studies shown in Tables 2–4.

It has been shown that salicylanilides form stable intermolecular hydrogen bonds, resulting in rigid, planar conformations.³⁷ This is likely the case for compounds **6c** and **6f**. However, in all other compounds that contain electron withdrawing groups at the 3 and 5 positions of the A-ring, we predict that the hydroxyl is predominantly ionized at physiological pH. This ionized form may form an electron delocalized “pseudo-ring” with the amide nitrogen proton or may simply be absent of intramolecular hydrogen bonding. While the exact conformation that effectively inhibits PARG is not currently known, it is likely that the negative

Table 5. Cross-Inhibition with PARP-1

compd	PARG IC ₅₀ (μM)	PARP-1 IC ₅₀ (μM)
1e	8 ± 0.6	123 ± 19
1f	22 ± 2	22 ± 6
1g	26 ± 3	78 ± 14
6a	12 ± 2	120 ± 22
6g	72 ± 7	66 ± 6
8b	261 ± 75	~500
8c	~500	~500
ADP-HPD ^a	0.12	>1000
benzamide ^b	>1000	5.4 ± 0.4

^a See ref 30. ^b See ref 38.

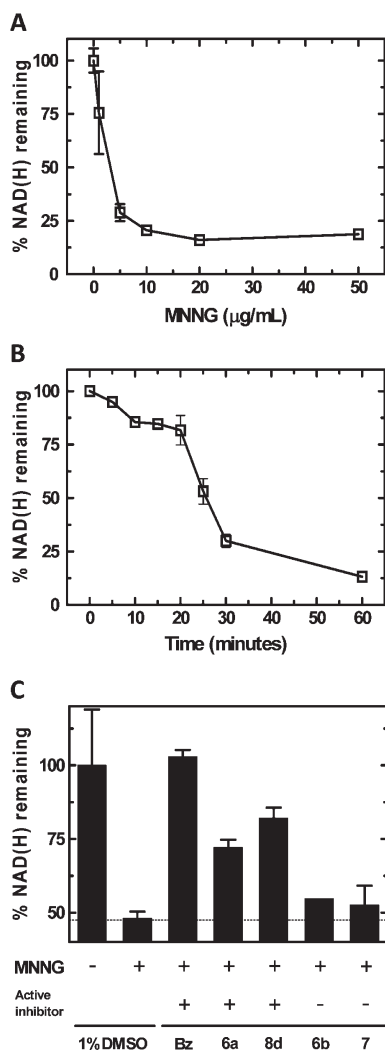


Figure 2. Depletion of NAD(H) in SCC-25 cells following genotoxic stress: (A) treatment with varying concentrations of MNNG for 30 min; (B) time course of NAD(H) levels following treatment with MNNG (5 μg/mL); (C) effects on NAD(H) depletion in cells treated with MNNG (5 μg/mL) for 30 min, pretreated with 1 mM of benzamide (Bz), 6a, 8d, 6b, or 7.

charge plays a key role in inhibition, since the PAR substrate of PARG is a large, highly negatively charged polymer. It is possible that the anionic hydroxyl (or carboxylic acid 6g) mimics the negatively charged characteristic of PAR.

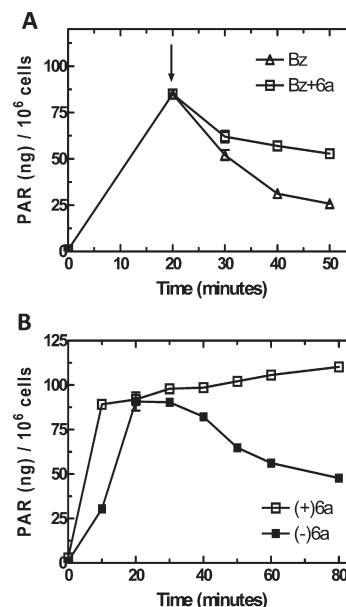


Figure 3. PAR formation in SCC-25 cells following genotoxic stress: (A) time course of PAR formation after treatment of MNNG (5 μg/mL), where cells were treated with 1 mM benzamide with compound 6a (□) and without compound 6a (Δ) at 20 min as indicated by the arrow; (B) time course of PAR formation following treatment of MNNG (5 μg/mL), pretreated with 1 mM compound 6a (□) and without pretreatment (■).

PARG Inhibitors Also Show Inhibition of PARP-1. We next examined the selectivity of compounds containing the PARG pharmacophore. Recent secondary structure predictions suggest that the active site domain of PARG has a high degree of homology to the ADP-ribosyl transferase domain of PARPs.³⁸ Accordingly, we examined a number of the PARG inhibitors described in Tables 1–4 for effects on PARP-1. Each of these compounds also showed significant inhibition of PARP-1 (Table 5), although one compound 1e had a PARG selectivity of 15-fold. Also included in Table 5 are values taken from previous studies showing that the PARG inhibitor ADP-HPD does not inhibit PARP-1³⁰ and conversely that the PARP inhibitor benzamide does not inhibit PARG,³⁹ demonstrating that selective inhibition of these two enzymes can be achieved. The PARG inhibitors did not inhibit the activity of other NAD⁺ binding enzymes that bind via other NAD⁺ binding motifs, SIRT1 and alcohol dehydrogenase (data not shown). The results shown in Table 5 point out a significant future challenge for the development of PARG specific inhibitors. On the other hand, they describe the discovery of a novel class of inhibitors with the potential to disrupt the coordination of PARP and PARG activities needed for cell responses to DNA damage.

PARG Inhibitors Inhibit Both PARP and PARG in Intact Cells but Show a Preference for PARG Inhibition. The efficacy of lead compounds was assessed by examining effects on PARP and PARG activity in a squamous cell carcinoma cell line (SCC-25). Effects on PARP activity in cells were examined by determination of NAD(H) depletion following treatment with the DNA damaging agent *N*-methyl-*N*-nitro-*N*-nitrosoguanidine (MNNG) as shown in Figure 2. When cells were treated for 30 min with MNNG, a dose-dependent decrease in NAD(H) content was observed (Figure 2A). The depletion of NAD(H) after 5 μg/mL MNNG treatment occurred for about 30 min, at which point consumption began to level off (Figure 2B). The

complete inhibition of NAD(H) depletion by preincubation with the PARP inhibitor benzamide (Figure 2C) demonstrates that the depletion represents PARP activity in intact cells. Treatment of cells with active compounds **6a** and **8d** resulted in partial inhibition of NAD(H) consumption, while treatment with inactive compounds **6b** and **7** had minimal effect (Figure 2C). For all compounds, a concentration of 1 mM was utilized for proof of principle of cell permeability. These results of Figure 2 demonstrate that **6a** and **8d** are causing PARP inhibition in intact cells. However, it is not possible to distinguish between direct inhibition of PARP activity and indirect inhibition due to increased automodification secondary to PARG inhibition.

To examine for effects on PARG activity in intact cells, PAR turnover experiments were completed. SCC-25 cells were first treated with MNNG to induce PAR formation. The addition of 1 mM benzamide at 20 min inhibits further PARP activity; thus, decreases in PAR content are due exclusively to PARG activity (Figure 3A). When 1 mM **6a** was added along with benzamide, PAR turnover was strongly inhibited following a short lag period (Figure 3A). These data further demonstrate that **6a** effectively inhibits PARG in intact cells.

To examine the relative inhibition of **6a** on PARP and PARG in SCC-25 cells, PAR content following MNNG treatment was examined in the presence and absence of **6a**. The activities of PARP and PARG are closely coordinated; thus, the levels of PAR over time represent the relative activities of PARP and PARG. At the dose of MNNG used, PAR levels rapidly rise and reach a plateau at approximately 20 min and then slowly decline as PAR turnover continues but NAD(H) substrate is depleted (Figure 3B). When cells were preincubated with **6a**, PAR accumulation at 10 min was increased approximately 3-fold and PAR levels continued to increase gradually over the course of the experiment (Figure 3B). These results demonstrate a preferential inhibition of PARG over PARP by **6a**. The same conclusion can be drawn from the results observed on PARP and PARG activity separately where **6a** showed approximately 40% inhibition of PARP activity (Figure 2C) but nearly complete inhibition of PARG (Figure 3B) under the conditions of the experiments.

Implications for Therapeutic Development. The close coordination of PARP and PARG activities required for cellular responses to DNA damage and the results of clinical trials of PARP inhibitors for cancer treatment that report both low toxicity and promising efficacy¹⁴ dictate an evaluation of the therapeutic potential of PARG for cancer therapy. Additionally, the therapeutic potential of targeting PAR metabolism extends beyond cancer therapy to other pathological conditions that result from acute or chronic genotoxic stress. Upon DNA strand break recognition, PARP-1 activity is elevated nearly 500-fold.⁴⁰ High levels of DNA damage lead to concerted PARP and PARG activity that in turn results in rapid cellular depletion of NAD(H) and release of mitochondrial components that promote cell death.^{41,42} Protective effects seen with PARP inhibition have therapeutic implications that include chronic heart disease, diabetic cardiovascular complications, circulatory shock, neurological diseases, ischemia/reperfusion injury, and Parkinson's disease.^{43–45} PARP-1 activity is negatively regulated by PAR automodification and PARG is required for removing automodification.¹⁷ Thus, inhibition of PARG potentially represents an approach to prevent cell death by indirect inhibition of PARP activity.

Previously, a number of studies have reported positive effects in model systems of **13**, a member of a group of symmetrically disubstituted aromatic PARG inhibitors developed by Guilford

Pharmaceuticals, Inc.^{32,46,47} However, the cell permeability and selectivity of this class of inhibitors have not been reported. While we have demonstrated cellular activity of the lead PARG inhibitors described here, the observation that these inhibitors also inhibit PARP-1 in vitro and PARP activity in intact cells raises a new challenge for the development of PARG selective inhibitors. While the lead PARG inhibitors described here are not completely selective for PARG, the high degree of selectivity of inhibitors such as ADP-HPD for PARG³⁰ provides evidence that future SAR studies have the potential to lead to highly selective and cell permeable PARG inhibitors. While more research is needed, the current PARG inhibitors show a more potent inhibition of PARG than PARP in intact cells (Figures 2 and 3). Indeed, while it is possible to determine effects on PARG activity in the absence of PARP activity (Figure 3A), inhibition of PARP activity in intact cells can be due to both direct inhibition of PARP and indirect inhibition of PARP as a result of increased automodification that inhibits PARP activity secondary to PARG inhibition.¹⁷

Our results, together with other work from our laboratory,³⁸ make it likely that the active sites of PARG and PARP-1 (and likely other PARPs) share a high degree of similarity. Inhibition of PARG is not observed with PARP inhibitors such as benzamide that target the nicotinamide binding pocket of the NAD⁺ binding site of PARPs,³⁹ as PARG most likely does not contain such a site. However, current highly potent PARP inhibitors are designed to reach outside the nicotinamide binding pocket into the ADP-ribose region of the NAD⁺ site to gain favorable ADME properties and selectivity among PARPs.¹¹ This added bulkiness of current PARP-1 inhibitors raises the possibility of PARG cross-inhibition. PARG inhibition may not be a concern with highly potent PARP inhibitors specific for a particular cellular PARP but could possibly cause off target effects related to altered regulation of the coordinate function of a nontarget PARP with its specific PARG partner. Consequently, the possible effect of current PARP clinical candidates on PARG would be of interest.

The molecules reported here represent only the initial steps in the development of molecules that will allow the evaluation of the therapeutic potential of targeting PARG. The current molecules provide proof of principle that cell permeable PARG inhibitors can be developed, but further studies will be needed to provide a definitive assessment of general toxicity and therapeutic potential of PARG inhibition.

CONCLUSIONS

The identification of several small molecule inhibitors of PARG has been obtained using a novel screening technology. Analogues based on these screening hits were designed to determine SAR that led to a modified salicylanilide pharmacophore for PARG inhibition. Analysis of the A-ring reveals an acidic hydroxyl as a key feature necessary for PARG inhibition. Further analysis of the amide linker reveals that a HBD is essential for PARG inhibition and a HBA is favorable for PARG inhibition. A B-ring is required for inhibition, and a hydrophobic substituent on the B-ring is highly favorable. The C-ring contributes greatly to potency, even though the extra size is not favorable in terms of obtaining desirable druglike properties. The cross-inhibition observed with PARP-1 is most likely attributed to the similarities of substrates in the active sites of both enzymes. Furthermore, **5a** demonstrated cell permeability for both PARP and PARG inhibition in intact cells. These studies point to future challenges for obtaining inhibitors highly selective for PARG. At

the same time, inhibitors that disrupt PAR metabolism via effects on both cellular PARPs and PARG may represent a new approach for the therapeutic targeting of PAR metabolism.

EXPERIMENTAL SECTION

Reagents. High specific activity (22,833 U/mg) PARP-1 was from Trevigen Inc. (Gaithersburg, MD). [32 P]NAD⁺ was from Perkin-Elmer (Waltham, MA). All rPARG-CF was prepared as a 3.3 mg/mL stock as previously described.⁴⁸

PARP Assay. This assay utilizes the conditions previously reported.⁴⁹ Reaction mixtures were prepared in a 1.5 mL microfuge tube by adding 10 μ L of 3 \times glyco assay buffer (150 mM potassium phosphate buffer, pH 7.5, 150 mM KCl, 0.3 mg/mL BSA, and 30 mM 2-mercaptoethanol), 5 μ L of 60 μ M [α - 32 P]ADP-ribose polymers (approximately 5000 cpm/ μ L), 7 μ L of deionized water, and 3 μ L of test inhibitor in 50% DMSO. The reaction was initiated by the addition of 5 μ L of PARG (0.3 μ g/mL), and the reaction mixture was incubated at 37 $^{\circ}$ C for 5 min. The reaction was then stopped by the addition of 3 μ L of 1% SDS. Next, 3 μ L of the reaction mixture was loaded onto a 2 \times 10 cm poly(ethyleneimine)-cellulose F TLC plate, prespotted with 1 μ L of 10 mM ADP-ribose. The spot was dried, and the plate was placed into a TLC tank with 100 mL of methanol and developed until the solvent front reached the top of the plate. Next, the plate was transferred into a second tank containing 100 mL of a solution comprising 0.9 M acetic acid and 0.3 M LiCl. After the plate was developed as before, it was air-dried and the ADP-ribose spot was visualized by using a hand-held short-wave UV lamp. The origin and ADP-ribose spot were excised, placed into 20 mL scintillation vials with 10 mL of EcoLume added, and the radioactivity was counted in a Beckman liquid scintillation counter.

PARP-1 Assay. PARP-1 was diluted by PARP dilution buffer containing 50 mM Tris-HCl (pH 8.0), 1 mM DTT, 4 mM MgCl₂, 1 mM PMSF, 2 μ g/mL aprotinin, and 0.3 mg/mL BSA. The reaction was initiated by addition of PARP-1 to the PARP reaction mixture containing 100 mM Tris-HCl (pH 8.0), 10 mM MgCl₂, 2 mM DTT, 5 μ g of histone H1, 5 μ g of activated DNA, 0.1 mM NAD⁺, and 50 000 cpm [32 P]NAD⁺. The incubation time was 15 min. The reaction was terminated by addition of 12.5 μ L of ice-cold 100% TCA. Then 5 μ L of BSA (10 mg/mL) was added and the mixture was cooled at -20 $^{\circ}$ C for 10 min before a 15 min centrifugation at 4 $^{\circ}$ C and 14 000 rpm. The supernatant was collected, and the pellet was washed with 100 μ L of 20% TCA and subjected to a second centrifugation for 15 min at 4 $^{\circ}$ C at 14 000 rpm. The supernatant was collected as the wash and the pellet was suspended in 100 μ L of 88% formic acid and collected as the pellet.

NAD Assay. The NAD recycling assay as described by Jacobson and Jacobson was followed with minor adjustments.⁵⁰ Briefly, 90% confluent SCC-25 cells in 35 mm dishes were pretreated for 5 min with test compound before being treated with 5 μ g/mL MNNG. After 30 min the medium was removed and washed with 1 mL of PBS twice before being treated with 0.2 mL of ice-cold 0.5 M HClO₄. Cells were scraped from the dish and washed with an additional 0.2 mL of HClO₄. Cell extracts were then centrifuged at 14 000 rpm for 10 min at 4 $^{\circ}$ C. Supernatants were neutralized with 135 μ L of 2 M KOH/0.66 M KH₂PO₄ (to adjust pH to 7.0–7.5) and used for the measurement of NAD. The KClO₄ precipitate was removed, and 20 μ L of the supernatant was incubated for 30 min at 37 $^{\circ}$ C with 2 mM phenazine ethosulfate, 0.5 mM 3-(4,5-dimethylthiazol-2-yl)-2,5-diphenyltetrazolium bromide, 50 mM EDTA, 600 mM ethanol, and 120 mM bicine, pH 7.8, and alcohol dehydrogenase (50 μ g/mL, Sigma) in a 96-well plate. Absorbance was determined at 570 nm using a VERSAmix plate reader. Detected NAD content was normalized to cell protein content.

PAR Assay. High throughput chemiluminescent ELISA (HT PARP in vivo pharmacodynamic assay II developed by Trevigen) was used to

quantify ADP-ribose polymers in adherent cultured cells. The procedure followed was according to the supplied protocol, with minor adjustments. Briefly, 90% confluent SCC-25 cells in 35 mm dishes were treated with 5 μ g/mL MNNG. Cells were harvested by addition of lysis buffer containing 1% SDS. Detected PAR levels were normalized to cell count.

SAR Studies. Inhibition assays were performed in duplicate with selected inhibitors in 5% DMSO. The catalytic activity of PARG and PARP-1 was measured in the presence of varying concentrations of inhibitors. Data were fit to the equation describing a sigmoidal dose response relation between % activity (from 100 to 0) and log[inhibitor] using GraphPad Prism, version 4, for Windows (GraphPad Software, San Diego, CA, www.graphpad.com). The procedure resulted in calculated values for log IC₅₀ and standard error, which are reported.

Chemistry. Starting materials were purchased from Aldrich and Alfa-Aesar and used without further purification unless otherwise specified. Flash column chromatography was performed on silica gel (200–400 mesh, 60 Å), eluting with CH₂Cl₂. Proton (1 H NMR) nuclear magnetic resonance spectra were recorded on a Bruker Avance spectrometer at 300 MHz. Chemical shifts (δ) are in parts per million (ppm) relative to Si(CH₃)₄, and coupling constants (J) are in hertz. The NMR solvent used was DMSO-*d*₆. For routine aqueous workup, the reaction mixture was extracted with CH₂Cl₂ or EtOAc. The organic layer was washed twice with Na₂HCO₃, once with brine, dried over anhydrous MgSO₄, and concentrated with a Büchi rotary evaporator. All compounds tested in assays were >95% pure as determined by RP-HPLC, using 0.5% TFA (aq)/MeOH (2:8) elution phase.

General Procedure for the Synthesis of Compounds

2a–g. To selected nitrobenzenes (4 mmol) in toluene were added substituted phenols (6 mmol, 1.5 equiv) and Cs₂CO₃ (12 mmol, 3 equiv), and the mixture was left stirring under nitrogen. The reaction was kept at 100 $^{\circ}$ C and left until completion (24–36 h). The reaction progress was monitored by TLC (15% EtOAc/hexane), and once all nitroaryl halide was reacted, the solvent was removed in vacuo and redissolved in EtOAc. The mixture was then filtered, and routine aqueous workup was performed on the filtrate. The organic phase was concentrated and purified by column chromatography (5% EtOAc/hexane) to obtain compounds **2a–g** as red and yellow oils.

2-(2-Chloro-4-nitrophenoxy)naphthalene (2a). Yield 57%; R_f = 0.60 (15% EtOAc/hexane); 1 H NMR (300 MHz, DMSO-*d*₆) δ 8.48 (d, J = 2.7 Hz, 1H), 8.16 (dd, J = 9.1, 2.8 Hz, 1H), 8.07 (d, J = 8.9 Hz, 1H), 7.99 (d, J = 7.1 Hz, 1H), 7.90 (d, J = 7.0 Hz, 1H), 7.67 (d, J = 2.0 Hz, 1H), 7.54 (tt, J = 6.9, 5.3 Hz, 2H), 7.40 (dd, J = 8.9, 2.4 Hz, 1H), 7.12 (d, J = 9.1 Hz, 1H).

2-(4-Nitrophenoxy)naphthalene (2b). Yield 52%; R_f = 0.67 (15% EtOAc/hexane); 1 H NMR (300 MHz, DMSO-*d*₆) δ 8.27 (d, J = 9.2 Hz, 2H), 8.07 (d, J = 8.9 Hz, 1H), 8.00 (d, J = 7.0 Hz, 1H), 7.92 (d, J = 7.4 Hz, 1H), 7.71 (d, J = 2.2 Hz, 1H), 7.55 (m, 2H), 7.39 (dd, J = 8.9, 2.4 Hz, 1H), 7.21 (d, J = 9.2 Hz, 2H).

2-(2-Fluoro-4-nitrophenoxy)naphthalene (2c). Yield 58%; R_f = 0.45 (15% EtOAc/hexane); 1 H NMR (300 MHz, DMSO-*d*₆) δ 8.37 (dd, J = 10.8, 2.7 Hz, 1H), 8.10 (d, J = 2.7 Hz, 1H), 8.06 (d, J = 8.8 Hz, 1H), 7.98 (d, J = 7.3 Hz, 1H), 7.89 (d, J = 7.2 Hz, 1H), 7.66 (d, J = 2.0 Hz, 1H), 7.53 (m, 2H), 7.42 (dd, J = 8.9, 2.4 Hz, 1H), 7.25 (d, J = 8.4 Hz, 1H).

2-(4-Nitro-2-(trifluoromethyl)phenoxy)naphthalene (2d). Yield 66%; R_f = 0.70 (15% EtOAc/hexane); 1 H NMR (300 MHz, DMSO-*d*₆) δ 8.55 (d, J = 2.6 Hz, 1H), 8.45 (dd, J = 9.2, 2.7 Hz, 1H), 8.11 (d, J = 8.9 Hz, 1H), 8.02 (d, J = 6.6 Hz, 1H), 7.95 (d, J = 7.0 Hz, 1H), 7.79 (d, J = 2.2 Hz, 1H), 7.58 (m, 2H), 7.41 (dd, J = 8.9, 2.0 Hz, 1H), 7.18 (d, J = 9.2 Hz, 1H).

2-(2-Methyl-4-nitrophenoxy)naphthalene (2e). Yield 43%; R_f = 0.54 (15% EtOAc/hexane); 1 H NMR (300 MHz, DMSO-*d*₆) δ 8.27 (d, J = 2.6 Hz, 1H), 8.05 (dd, J = 8.8, 4.1 Hz, 2H), 7.97 (d, J = 7.2 Hz, 1H), 7.87 (d, J = 6.9 Hz, 1H), 7.57 (d, J = 1.9 Hz, 1H), 7.52 (m, 2H), 7.35 (dd, J = 8.9, 2.4 Hz, 1H), 6.93 (d, J = 9.0 Hz, 1H), 2.41 (s, 3H).

2-Chloro-4-nitro-1-(*p*-tolylxy)benzene (**2f**). Yield 58%; $R_f = 0.65$ (15% EtOAc/hexane); $^1\text{H NMR}$ (300 MHz, DMSO- d_6) δ 8.42 (d, $J = 2.7$ Hz, 1H), 8.14 (dd, $J = 9.2, 2.8$ Hz, 1H), 7.30 (d, $J = 8.4$ Hz, 2H), 7.08 (d, $J = 8.4$ Hz, 2H), 6.94 (d, $J = 9.2$ Hz, 1H), 2.33 (s, 3H).

2-Chloro-4-nitro-1-phenoxybenzene (**2g**). Yield 68%; $R_f = 0.56$ (15% EtOAc/hexane); $^1\text{H NMR}$ (300 MHz, DMSO- d_6) δ 8.46 (d, $J = 2.7$ Hz, 1H), 8.18 (dd, $J = 9.1, 2.7$ Hz, 1H), 7.51 (t, $J = 7.8$ Hz, 1H), 7.32 (t, $J = 7.6$ Hz, 1H), 7.19 (d, $J = 7.8$ Hz, 1H), 7.15 (t, $J = 7.8$ Hz, 1H), 7.02 (d, $J = 9.1$ Hz, 1H), 6.74 (d, $J = 7.9$ Hz, 1H).

General Procedure for the Synthesis of Compounds 3a–g. To **2a–g** (3.0 mmol) dissolved in absolute ethanol and purged with nitrogen was added SnCl_2 (15.0 mmol, 5 equiv), and the mixture was left stirring at 70 °C. Reaction completion was monitored by TLC (CH_2Cl_2), and extra SnCl_2 was added as needed. Once completed (usually 3 h), the solvent was removed in vacuo and the sample was redissolved in EtOAc. The mixture was poured onto ice and the pH adjusted to 9.0 with 6 M NaOH. This mixture was then filtered, and routine aqueous workup was performed. The organic phase was concentrated and purified by column chromatography (CH_2Cl_2) to obtain **3a–g** as yellow-orange oils.

3-Chloro-4-(naphthalen-2-yloxy)aniline (**3a**). Yield 55%; $R_f = 0.35$ (CH_2Cl_2); $^1\text{H NMR}$ (300 MHz, DMSO- d_6) δ 7.91 (d, $J = 9.0$ Hz, 1H), 7.87 (d, $J = 8.1$ Hz, 1H), 7.75 (d, $J = 8.1$ Hz, 1H), 7.41 (dt, $J = 14.7, 6.8$ Hz, 2H), 7.24 (dd, $J = 9.0, 1.8$ Hz, 1H), 7.01 (d, $J = 3.3$ Hz, 1H), 6.99 (d, $J = 5.0$ Hz, 1H), 6.76 (d, $J = 1.8$ Hz, 1H), 6.60 (dd, $J = 8.6, 1.8$ Hz, 1H), 5.38 (s, 2H).

4-(Naphthalen-2-yloxy)aniline (**3b**). Yield 45%; $R_f = 0.40$ (CH_2Cl_2); $^1\text{H NMR}$ (300 MHz, DMSO- d_6) δ 7.87 (d, $J = 9.2$ Hz, 1H), 7.84 (d, $J = 8.8$ Hz, 1H), 7.71 (d, $J = 7.8$ Hz, 1H), 7.39 (dt, $J = 20.1, 6.7$ Hz, 2H), 7.24 (dd, $J = 8.9, 2.5$ Hz, 1H), 7.13 (d, $J = 2.4$ Hz, 1H), 6.86 (d, $J = 8.7$ Hz, 2H), 6.66 (d, $J = 8.7$ Hz, 2H), 5.04 (s, 2H).

3-Fluoro-4-(naphthalen-2-yloxy)aniline (**3c**). Yield 61%; $R_f = 0.35$ (CH_2Cl_2); $^1\text{H NMR}$ (300 MHz, DMSO- d_6) δ 7.90 (d, $J = 9.1$ Hz, 1H), 7.87 (d, $J = 10.4$ Hz, 1H), 7.76 (d, $J = 8.1$ Hz, 1H), 7.41 (dt, $J = 20.4, 6.8$ Hz, 2H), 7.26 (dd, $J = 8.9, 2.5$ Hz, 1H), 7.07 (d, $J = 2.2$ Hz, 1H), 6.98 (d, $J = 9.1$ Hz, 1H), 6.53 (dd, $J = 13.3, 2.5$ Hz, 1H), 6.43 (dd, $J = 8.7, 1.7$ Hz, 1H), 5.39 (s, 2H).

4-(Naphthalen-2-yloxy)-3-(trifluoromethyl)aniline (**3d**). Yield 55%; $R_f = 0.44$ (CH_2Cl_2); $^1\text{H NMR}$ (300 MHz, DMSO- d_6) δ 7.90 (d, $J = 9.3$ Hz, 1H), 7.87 (d, $J = 10.0$ Hz, 1H), 7.77 (d, $J = 6.7$ Hz, 1H), 7.42 (m, 2H), 7.22 (dd, $J = 9.1, 2.3$ Hz, 1H), 7.14 (d, $J = 2.0$ Hz, 1H), 6.97 (d, $J = 6.0$ Hz, 1H), 6.95 (d, $J = 2.2$ Hz, 1H), 6.85 (dd, $J = 8.8, 2.2$ Hz, 1H), 5.50 (s, 2H).

2-(2-Methyl-4-nitrophenoxy)naphthalene (**3e**). Yield 59%; $R_f = 0.29$ (CH_2Cl_2); $^1\text{H NMR}$ (300 MHz, DMSO- d_6) δ 7.91 (d, $J = 9.0$ Hz, 1H), 7.86 (d, $J = 8.0$ Hz, 1H), 7.72 (d, $J = 8.3$ Hz, 1H), 7.40 (dt, $J = 14.7, 6.9$ Hz, 2H), 7.24 (dd, $J = 8.8, 2.2$ Hz, 1H), 7.00 (d, $J = 1.6$ Hz, 1H), 6.84 (d, $J = 8.4$ Hz, 1H), 6.71 (d, $J = 2.0$ Hz, 1H), 6.64 (dd, $J = 8.2, 1.9$ Hz, 1H), 6.54 (br s, 2H).

3-Chloro-4-(*p*-tolylxy)aniline (**3f**). Yield 47%; $R_f = 0.40$ (CH_2Cl_2); $^1\text{H NMR}$ (300 MHz, DMSO- d_6) δ 7.09 (d, $J = 8.4$ Hz, 2H), 6.86 (d, $J = 8.3$ Hz, 1H), 6.70 (d, $J = 1.7$ Hz, 1H), 6.69 (d, $J = 8.1$ Hz, 2H), 6.53 (dd, $J = 8.7, 1.7$ Hz, 1H), 5.29 (s, 2H), 2.23 (s, 3H).

3-Chloro-4-phenoxyaniline (**3g**). Yield 52%; $R_f = 0.27$ (CH_2Cl_2); $^1\text{H NMR}$ (300 MHz, DMSO- d_6) δ 7.30 (t, $J = 7.2$ Hz, 2H), 7.00 (t, $J = 7.3$ Hz, 1H), 6.90 (d, $J = 8.7$ Hz, 1H), 6.79 (d, $J = 7.8$ Hz, 2H), 6.72 (d, $J = 2.6$ Hz, 1H), 6.55 (dd, $J = 8.7, 2.6$ Hz, 1H), 5.32 (s, 2H).

3,5-Dichloro-2-methoxybenzoic Acid (**4**). To 1.2 g (5.8 mmol) of 3,5-dichlorosalicylic acid and 3 g (21.7 mmol, 3.7 equiv) of K_2CO_3 in 20 mL of acetone was added 1 mL (17.7 mmol, 3 equiv) of iodomethane, and the mixture was refluxed overnight. After 24 h the solution was cooled to room temperature. Then 10 mL of methanol was added followed by 5 mL of 6 M NaOH, and the mixture was further refluxed for 3 h. The solution was acidified by the addition of 6 M HCl until pH 1 was

reached. The precipitate was filtered and collected to obtain **4** as a pure white solid (80%). $R_f = 0.72$ (10% MeOH/ CHCl_3); $^1\text{H NMR}$ (300 MHz, DMSO- d_6) δ 13.58 (s, 1H), 7.88 (d, $J = 2.6$ Hz, 1H), 7.67 (d, $J = 2.5$ Hz, 1H), 3.82 (s, 3H).

General Procedure for the Synthesis of Compounds 5a–f. Corresponding benzoic acids were heated at 110 °C in thionyl chloride for 1–2 h. After completion, excess thionyl chloride was removed in vacuo. The product mixture was dissolved in CH_2Cl_2 and filtered. Filtrates were concentrated and used without further purification.

General Procedure for the Synthesis of Compounds 6a–m. To a stirred solution of amines **3a–g** (0.2 mmol) in 5 mL of CH_2Cl_2 was added benzoic acid chlorides **5a–f** or phthalamic anhydride (0.2 mmol, 1 equiv), and the reaction mixture was stirred at room temperature for 0.5 h. The reaction was monitored by TLC (CH_2Cl_2), and once completed, the mixture was concentrated and purified by column chromatography (CH_2Cl_2) to obtain **6a–m** as off-white solids.

3,5-Dichloro-*N*-(3-chloro-4-(naphthalen-2-yloxy)phenyl)-2-hydroxybenzamide (**6a**). Yield 65%; $R_f = 0.78$ (CH_2Cl_2); $^1\text{H NMR}$ (300 MHz, DMSO- d_6) δ 12.49 (br s, 1H), 10.77 (s, 1H), 8.09 (d, $J = 2.3$ Hz, 1H), 8.07 (d, $J = 2.3$ Hz, 1H), 7.98 (d, $J = 9.0$ Hz, 1H), 7.91 (d, $J = 7.4$ Hz, 1H), 7.81 (d, $J = 2.5$ Hz, 1H), 7.81 (d, $J = 5.5$ Hz, 1H), 7.70 (dd, $J = 8.8, 2.3$ Hz, 1H), 7.46 (m, 2H), 7.32 (dd, $J = 9.0, 2.4$ Hz, 1H), 7.28 (d, $J = 9.3$ Hz, 1H), 7.26 (d, $J = 2.4$ Hz, 1H). MS (ESI) m/z : 457.9 [$\text{M} + \text{H}$] $^+$.

3,5-Dichloro-*N*-(3-chloro-4-(naphthalen-2-yloxy)phenyl)benzamide (**6b**). Yield 57%; $R_f = 0.78$ (CH_2Cl_2); $^1\text{H NMR}$ (300 MHz, DMSO- d_6) δ 10.63 (s, 1H), 8.14 (t, $J = 2.1$ Hz, 1H), 8.01 (d, $J = 1.9$ Hz, 1H), 8.00 (d, $J = 1.9$ Hz, 1H), 8.00 (d, $J = 1.9$ Hz, 1H), 7.95 (d, $J = 11.0$ Hz, 1H), 7.90 (d, $J = 1.8$ Hz, 1H), 7.82 (d, $J = 8.0$ Hz, 1H), 7.76 (dd, $J = 8.9, 2.3$ Hz, 1H), 7.46 (td, $J = 14.7, 7.3$ Hz, 2H), 7.32 (d, $J = 9.1$ Hz, 1H), 7.29 (dd, $J = 8.9, 2.0$ Hz, 1H), 7.23 (s, 1H). MS (ESI) m/z : 441.9 [$\text{M} + \text{H}$] $^+$.

N-(3-Chloro-4-(naphthalen-2-yloxy)phenyl)-2-hydroxybenzamide (**6c**). Yield 43%; $R_f = 0.69$ (CH_2Cl_2); $^1\text{H NMR}$ (300 MHz, DMSO- d_6) δ 11.58 (s, 1H), 10.53 (s, 1H), 8.13 (s, 1H), 7.98 (d, $J = 8.8$ Hz, 1H), 7.92 (dd, $J = 7.9, 1.5$ Hz, 2H), 7.82 (d, $J = 7.9$ Hz, 1H), 7.71 (d, $J = 8.9$ Hz, 1H), 7.46 (m, 3H), 7.33 (d, $J = 8.9$ Hz, 1H), 7.28 (dd, $J = 8.9, 1.7$ Hz, 1H), 7.22 (s, 1H), 7.01 (d, $J = 9.6$ Hz, 1H), 6.98 (d, $J = 8.7$ Hz, 1H). MS (ESI) m/z : 390.0 [$\text{M} + \text{H}$] $^+$.

5-Chloro-*N*-(3-chloro-4-(naphthalen-2-yloxy)phenyl)-2-hydroxybenzamide (**6d**). Yield 67%; $R_f = 0.72$ (CH_2Cl_2); $^1\text{H NMR}$ (300 MHz, DMSO- d_6) δ 11.73 (br s, 1H), 10.56 (s, 1H), 8.12 (d, $J = 2.3$ Hz, 1H), 7.95 (d, $J = 9.1$ Hz, 1H), 7.93 (d, $J = 2.6$ Hz, 1H), 7.89 (d, $J = 7.9$ Hz, 1H), 7.79 (d, $J = 8.0$ Hz, 1H), 7.70 (dd, $J = 8.8, 2.3$ Hz, 1H), 7.47 (dd, $J = 5.0, 3.8$ Hz, 1H), 7.45 (m, 2H), 7.31 (dd, $J = 8.9, 2.4$ Hz, 1H), 7.26 (d, $J = 8.9$ Hz, 1H), 7.22 (d, $J = 2.1$ Hz, 1H), 7.03 (d, $J = 8.8$ Hz, 1H). MS (ESI) m/z : 424.0 [$\text{M} + \text{H}$] $^+$.

3-Chloro-*N*-(3-chloro-4-(naphthalen-2-yloxy)phenyl)-2-hydroxybenzamide (**6e**). Yield 50%; $R_f = 0.72$ (CH_2Cl_2); $^1\text{H NMR}$ (300 MHz, DMSO- d_6) δ 12.45 (s, 1H), 10.76 (s, 1H), 8.08 (s, 1H), 7.99 (d, $J = 8.5$ Hz, 2H), 7.92 (d, $J = 7.5$ Hz, 1H), 7.83 (d, $J = 7.7$ Hz, 1H), 7.70 (t, $J = 9.9$ Hz, 2H), 7.47 (m, 2H), 7.33 (d, $J = 10.4$ Hz, 1H), 7.29 (d, $J = 11.5$ Hz, 1H), 7.26 (d, $J = 5.1$ Hz, 1H), 7.03 (t, $J = 7.3$ Hz, 1H). MS (ESI) m/z : 424.0 [$\text{M} + \text{H}$] $^+$.

3,5-Dichloro-*N*-(3-chloro-4-(naphthalen-2-yloxy)phenyl)-2-methoxybenzamide (**6f**). Yield 55%; $R_f = 0.67$ (CH_2Cl_2); $^1\text{H NMR}$ (300 MHz, DMSO- d_6) δ 10.75 (s, 1H), 8.12 (d, $J = 2.5$ Hz, 1H), 7.97 (d, $J = 9.0$ Hz, 1H), 7.91 (d, $J = 7.8$ Hz, 1H), 7.85 (d, $J = 2.6$ Hz, 1H), 7.81 (d, $J = 7.9$ Hz, 1H), 7.67 (dd, $J = 7.0, 2.5$ Hz, 1H), 7.65 (d, $J = 1.8$ Hz, 1H), 7.45 (m, 2H), 7.32 (dd, $J = 9.4, 2.0$ Hz, 1H), 7.29 (d, $J = 7.5$ Hz, 1H), 7.22 (d, $J = 2.4$ Hz, 1H), 3.87 (s, 3H). MS (ESI) m/z : 470.1 [$\text{M} - \text{H}$] $^-$.

2-(3-Chloro-4-(naphthalen-2-yloxy)phenyl)carbamoylbenzoic Acid (**6g**). Yield 92%; $R_f = 0.22$ (10% MeOH/ CHCl_3); $^1\text{H NMR}$ (300 MHz, DMSO- d_6) δ 13.12 (s, 1H), 10.64 (s, 1H), 8.10 (d, $J = 2.4$ Hz, 1H), 7.97 (d, $J = 8.9$ Hz, 1H), 7.91 (d, $J = 7.8$ Hz, 2H), 7.83 (d, $J = 7.5$ Hz, 1H), 7.68 (d, $J = 7.3$ Hz, 1H), 7.61 (m, 3H), 7.46 (m, 2H), 7.32 (dd,

$J = 9.6, 3.2$ Hz, 1H), 7.28 (d, $J = 8.9$ Hz, 1H), 7.19 (d, $J = 2.4$ Hz, 1H). MS (ESI) m/z : 417.9 [M + H]⁺.

3,5-Dichloro-2-hydroxy-N-(4-(naphthalen-2-yloxy)phenyl)benzamide (6h). Yield 47%; $R_f = 0.60$ (CH₂Cl₂); ¹H NMR (300 MHz, DMSO-*d*₆) δ 12.82 (br s, 1H), 10.74 (s, 1H), 8.13 (d, $J = 2.4$ Hz, 1H), 7.98 (d, $J = 8.9$ Hz, 1H), 7.92 (d, $J = 7.7$ Hz, 1H), 7.84 (d, $J = 5.6$ Hz, 1H), 7.82 (d, $J = 2.1$ Hz, 1H), 7.74 (d, $J = 8.8$ Hz, 2H), 7.47 (m, 2H), 7.39 (d, $J = 2.2$ Hz, 1H), 7.32 (dd, $J = 8.9, 2.3$ Hz, 1H), 7.16 (d, $J = 8.8$ Hz, 2H). MS (ESI) m/z : 422.4 [M - H]⁻.

3,5-Dichloro-2-hydroxy-N-(3-fluoro-4-(naphthalen-2-yloxy)phenyl)-2-hydroxybenzamide (6i). Yield 57%; $R_f = 0.72$ (CH₂Cl₂); ¹H NMR (300 MHz, DMSO-*d*₆) δ 12.45 (br s, 1H), 10.92 (s, 1H), 8.05 (d, $J = 0.9$ Hz, 1H), 7.98 (d, $J = 8.8$ Hz, 1H), 7.92 (d, $J = 7.7$ Hz, 1H), 7.83 (d, $J = 1.8$ Hz, 1H), 7.82 (d, $J = 4.5$ Hz, 1H), 7.55 (dd, $J = 9.3, 1.7$ Hz, 1H), 7.46 (m, 2H), 7.36 (dd, $J = 2.5, 1.2$ Hz, 1H), 7.32 (d, $J = 9.0$ Hz, 1H), 7.29 (d, $J = 1.0$ Hz, 1H). MS (ESI) m/z : 440.3 [M - H]⁻.

3,5-Dichloro-2-hydroxy-N-(4-(naphthalen-2-yloxy)-3-(trifluoromethyl)phenyl)benzamide (6j). Yield 63%; $R_f = 0.67$ (CH₂Cl₂); ¹H NMR (300 MHz, DMSO-*d*₆) δ 12.40 (br s, 1H), 10.90 (s, 1H), 8.22 (d, $J = 2.2$ Hz, 1H), 8.08 (d, $J = 2.4$ Hz, 1H), 8.01 (d, $J = 9.1$ Hz, 1H), 7.97 (dd, $J = 2.3, 9.1$ Hz, 1H), 7.95 (d, $J = 7.1$ Hz, 1H), 7.87 (d, $J = 7.5$ Hz, 1H), 7.83 (d, $J = 2.4$ Hz, 1H), 7.50 (td, $J = 13.0, 6.0$ Hz, 2H), 7.47 (d, $J = 1.5$ Hz, 1H), 7.33 (dd, $J = 8.9, 2.5$ Hz, 1H), 7.23 (d, $J = 8.9$ Hz, 1H). MS (ESI) m/z : 490.3 [M - H]⁻.

3,5-Dichloro-2-hydroxy-N-(3-methyl-4-(naphthalen-2-yloxy)phenyl)benzamide (6k). Yield 64%; $R_f = 0.64$ (CH₂Cl₂); ¹H NMR (300 MHz, DMSO-*d*₆) δ 12.80 (br s, 1H), 10.70 (s, 1H), 8.14 (d, $J = 1.9$ Hz, 1H), 7.96 (d, $J = 9.1$ Hz, 1H), 7.90 (d, $J = 7.9$ Hz, 1H), 7.83 (d, $J = 2.2$ Hz, 1H), 7.78 (d, $J = 8.1$ Hz, 1H), 7.71 (d, $J = 1.6$ Hz, 1H), 7.58 (dd, $J = 8.8, 2.3$ Hz, 1H), 7.44 (dt, $J = 15.9, 6.9$ Hz, 2H), 7.29 (dd, $J = 8.9, 2.4$ Hz, 1H), 7.15 (d, $J = 1.7$ Hz, 1H), 7.06 (d, $J = 8.8$ Hz, 1H), 2.22 (s, 3H). MS (ESI) m/z : 436.2 [M - H]⁻.

3,5-Dichloro-N-(3-chloro-4-(p-tolyloxy)phenyl)-2-hydroxybenzamide (6l). Yield 51%; $R_f = 0.71$ (CH₂Cl₂); ¹H NMR (300 MHz, DMSO-*d*₆) δ 12.53 (br s, 1H), 10.69 (s, 1H), 8.07 (d, $J = 2.6$ Hz, 1H), 7.98 (d, $J = 2.6$ Hz, 1H), 7.78 (d, $J = 2.5$ Hz, 1H), 7.62 (dd, $J = 8.9, 2.6$ Hz, 1H), 7.18 (d, $J = 8.5$ Hz, 2H), 7.08 (d, $J = 8.9$ Hz, 1H), 6.86 (d, $J = 8.5$ Hz, 2H), 2.27 (s, 3H). MS (ESI) m/z : 422.1 [M + H]⁺.

3,5-Dichloro-N-(3-chloro-4-phenoxyphenyl)-2-hydroxybenzamide (6m). Yield 54%; $R_f = 0.56$ (CH₂Cl₂); ¹H NMR (300 MHz, DMSO-*d*₆) δ 12.42 (br s, 1H), 10.79 (s, 1H), 8.06 (d, $J = 2.9$ Hz, 1H), 8.02 (d, $J = 2.8$ Hz, 1H), 7.83 (d, $J = 2.8$ Hz, 1H), 7.65 (dd, $J = 8.9, 2.8$ Hz, 1H), 7.39 (t, $J = 7.7$ Hz, 2H), 7.18 (d, $J = 8.8$ Hz, 1H), 7.13 (t, $J = 7.0$ Hz, 1H), 6.96 (d, $J = 8.1$ Hz, 2H). MS (ESI) m/z : 408.2 [M - H]⁻.

3,5-Dichloro-2-hydroxybenzamide (7). To a stirred solution of ammonium hydroxide (2 mmol, 5 equiv) in 5 mL of CH₂Cl₂ was added salicylic acid chloride (0.4 mmol, 1 equiv), and the reaction mixture was stirred at room temperature for 30 min. The reaction was monitored by TLC (CH₂Cl₂), and once completed, the mixture was concentrated in vacuo and purified by column chromatography (CH₂Cl₂) to obtain 7 as a white solid. Yield 23%; $R_f = 0.60$ (10% MeOH/CHCl₃); ¹H NMR (300 MHz, DMSO-*d*₆) δ 14.15 (s, 1H), 8.70 (s, 1H), 8.33 (s, 1H), 8.00 (d, $J = 1.4$ Hz, 1H), 7.77 (d, $J = 1.3$ Hz, 1H). MS (ESI) m/z : 204.1 [M - H]⁻.

General Procedure for the Synthesis of Compounds 8a–h. To a stirred solution of selected anilines (0.3 mmol) in 5 mL of CH₂Cl₂ was added salicylic acid chloride (0.3 mmol, 1 equiv), and the reaction mixture was stirred at room temperature for 30 min. The reaction was monitored by TLC (CH₂Cl₂), and once completed, the mixture was concentrated in vacuo and purified by column chromatography (CH₂Cl₂) to obtain compounds 8a–h as off-white solids.

3,5-Dichloro-N-(3-chloro-4-hydroxyphenyl)-2-hydroxybenzamide (8a). Yield 58%; $R_f = 0.13$ (CH₂Cl₂); ¹H NMR (300 MHz, DMSO-*d*₆) δ 12.91 (br s, 1H), 10.59 (s, 1H), 8.15 (d, $J = 2.5$ Hz, 1H), 7.81 (d, $J = 2.4$ Hz, 1H), 7.73 (d, $J = 2.4$ Hz, 1H), 7.43 (dd, $J = 8.8, 2.5$ Hz, 1H), 7.01 (d, $J = 8.8$ Hz, 1H), 4.11 (s, 1H). MS (ESI) m/z : 330.3 [M - H]⁻.

3,5-Dichloro-N-(2-chlorophenyl)-2-hydroxybenzamide (8b). Yield 60%; $R_f = 0.75$ (CH₂Cl₂); ¹H NMR (300 MHz, DMSO-*d*₆) δ 12.82 (br s, 1H), 10.92 (s, 1H), 8.13 (d, $J = 2.5$ Hz, 1H), 7.87 (d, $J = 2.5$ Hz, 1H), 7.82 (d, $J = 7.9$ Hz, 1H), 7.60 (d, $J = 7.9$ Hz, 1H), 7.43 (t, $J = 7.7$ Hz, 1H), 7.33 (t, $J = 7.6$ Hz, 1H). MS (ESI) m/z : 314.2 [M - H]⁻.

3,5-Dichloro-N-(3-chlorophenyl)-2-hydroxybenzamide (8c). Yield 62%; $R_f = 0.70$ (CH₂Cl₂); ¹H NMR (300 MHz, DMSO-*d*₆) δ 12.39 (br s, 1H), 10.74 (s, 1H), 8.06 (d, $J = 2.5$ Hz, 1H), 7.87 (t, $J = 2.0$ Hz, 1H), 7.82 (d, $J = 2.5$ Hz, 1H), 7.63 (ddd, $J = 8.2, 1.9, 0.9$ Hz, 1H), 7.44 (t, $J = 8.1$ Hz, 1H), 7.26 (ddd, $J = 8.0, 2.1, 0.9$ Hz, 1H). MS (ESI) m/z : 314.2 [M - H]⁻.

3,5-Dichloro-N-(4-chlorophenyl)-2-hydroxybenzamide (8d). Yield 73%; $R_f = 0.70$ (CH₂Cl₂); ¹H NMR (300 MHz, DMSO-*d*₆) δ 12.53 (s, 1H), 10.72 (s, 1H), 8.11 (d, $J = 2.5$ Hz, 1H), 7.82 (d, $J = 2.4$ Hz, 1H), 7.73 (d, $J = 8.9$ Hz, 2H), 7.47 (d, $J = 8.9$ Hz, 2H). MS (ESI) m/z : 314.2 [M - H]⁻.

3,5-Dichloro-2-hydroxy-N-o-tolylbenzamide (8e). Yield 57%; $R_f = 0.69$ (CH₂Cl₂); ¹H NMR (300 MHz, DMSO-*d*₆) δ 13.10 (br s, 1H), 10.57 (s, 1H), 8.17 (d, $J = 1.6$ Hz, 1H), 7.85 (d, $J = 1.0$ Hz, 1H), 7.38 (d, $J = 6.6$ Hz, 1H), 7.32 (d, $J = 6.7$ Hz, 1H), 7.25 (m, 2H), 2.24 (s, 3H). MS (ESI) m/z : 294.3 [M - H]⁻.

3,5-Dichloro-2-hydroxy-N-m-tolylbenzamide (8f). Yield 71%; $R_f = 0.74$ (CH₂Cl₂); ¹H NMR (300 MHz, DMSO-*d*₆) δ 12.81 (br s, 1H), 10.59 (s, 1H), 8.17 (d, $J = 2.2$ Hz, 1H), 7.82 (d, $J = 2.2$ Hz, 1H), 7.53 (s, 1H), 7.49 (d, $J = 8.2$ Hz, 1H), 7.29 (t, $J = 7.7$ Hz, 1H), 7.02 (d, $J = 7.1$ Hz, 1H), 2.33 (s, 3H). MS (ESI) m/z : 294.2 [M - H]⁻.

3,5-Dichloro-2-hydroxy-N-p-tolylbenzamide (8g). Yield 66%; $R_f = 0.69$ (CH₂Cl₂); ¹H NMR (300 MHz, DMSO-*d*₆) δ 12.88 (br s, 1H), 10.56 (s, 1H), 8.18 (d, $J = 2.2$ Hz, 1H), 7.84 (d, $J = 2.3$ Hz, 1H), 7.38 (d, $J = 6.6$ Hz, 1H), 7.31 (d, $J = 2.9$ Hz, 1H), 7.25 (dd, $J = 6.4, 3.4$ Hz, 2H), 2.24 (s, 3H). MS (ESI) m/z : 294.3 [M - 1]⁻.

3,5-Dichloro-2-hydroxy-N-benzamide (8h). Yield 66%; $R_f = 0.69$ (CH₂Cl₂); ¹H NMR (300 MHz, DMSO-*d*₆) δ 12.78 (br s, 1H), 10.70 (s, 1H), 8.13 (d, $J = 2.2$ Hz, 1H), 7.82 (d, $J = 2.3$ Hz, 1H), 7.68 (d, $J = 8.4$ Hz, 2H), 7.41 (t, $J = 7.8$ Hz, 2H), 7.20 (t, $J = 7.5$ Hz, 1H). MS (ESI) m/z : 280.2 [M - 1]⁻.

2,4-Dichloro-6-((3-chloro-4-(naphthalen-2-yloxy)phenylimino)methyl)phenol (9). To a stirred solution of 100 mg (0.37 mmol) of 3a in 10 mL of ethanol was added 140 mg (0.74 mmol, 2 equiv) of 3,5-dichlorohydroxybenzaldehyde dissolved in 2 mL of methanol, and the reaction mixture was left stirring until a bright orange precipitate formed. The reaction was monitored by TLC (CH₂Cl₂), and once completed, the mixture was chilled to 4 °C. The precipitate was filtered and washed twice with 10 mL of ethanol to obtain 9 as an orange solid. Yield 90%; $R_f = 0.83$ (CH₂Cl₂); ¹H NMR (300 MHz, DMSO-*d*₆) δ 13.98 (s, 1H), 9.09 (s, 1H), 8.01 (d, $J = 9.7$ Hz, 1H), 7.94 (d, $J = 7.9$ Hz, 1H), 7.90 (d, $J = 2.5$ Hz, 1H), 7.84 (d, $J = 7.8$ Hz, 1H), 7.78 (d, $J = 2.6$ Hz, 1H), 7.74 (d, $J = 2.6$ Hz, 1H), 7.55 (dd, $J = 8.7, 2.5$ Hz, 1H), 7.48 (m, 2H), 7.36 (dd, $J = 6.6, 2.8$ Hz, 1H), 7.35 (d, $J = 3.1$ Hz, 1H), 7.31 (d, $J = 8.7$ Hz, 1H). MS (ESI) m/z : 440.3 [M - H]⁻.

2,4-Dichloro-6-((3-chloro-4-(naphthalen-2-yloxy)phenylamino)methyl)phenol (10). To a stirred solution of 50 mg (0.113 mmol) of 9 in 5 mL of methanol was added 113 μ L of 5 M sodium cyanoborohydride (0.565 mmol, 5 equiv), and the mixture was left stirring for 24 h at 70 °C. The reaction was monitored by TLC (CH₂Cl₂), and once completed, routine aqueous workup was performed. The organic phase was concentrated and purified by column chromatography (CH₂Cl₂) to obtain 10 as an orange solid. Yield 40%; $R_f = 0.76$ (CH₂Cl₂); ¹H NMR (300 MHz, DMSO-*d*₆) δ 9.78 (s, 1H), 7.91 (d, $J = 9.0$ Hz, 1H), 7.87 (d, $J = 8.0$ Hz, 1H), 7.74 (d, $J = 7.8$ Hz, 1H), 7.42 (d, $J = 2.5$ Hz, 1H), 7.41 (m, 2H), 7.25 (d, $J = 2.4$ Hz, 1H), 7.23 (dd, $J = 6.3, 2.6$ Hz, 1H), 7.07 (d, $J = 8.6$ Hz, 1H), 7.02 (d, $J = 2.4$ Hz, 1H), 6.77 (d, $J = 2.7$ Hz, 1H), 6.62 (dd, $J = 8.9, 2.7$ Hz, 1H), 6.49 (t, $J = 5.8$ Hz, 1H), 4.29 (d, $J = 5.6$ Hz, 2H). MS (ESI) m/z : 442.1 [M - H]⁻.

3-Chloro-*N*-methyl-4-(naphthalen-2-yloxy)aniline (**11**). To 100 mg (0.37 mmol) of **3a** and 510 mg (3.7 mmol, 10 equiv) of K_2CO_3 in 10 mL of acetone was added 23 μ L (0.37 mmol) iodomethane, and the mixture was refluxed for 1 h. Every hour 1 equiv of iodomethane was added and monitored by TLC until the starting material was consumed. The solvent was removed in vacuo, and routine aqueous workup was performed. The mixture was concentrated and purified by column chromatography (CH_2Cl_2) to obtain **11** as a white solid. Yield 29%; $R_f = 0.58$ (CH_2Cl_2); 1H NMR (300 MHz, DMSO- d_6) δ 7.91 (d, $J = 9.1$ Hz, 1H), 7.87 (d, $J = 8.2$ Hz, 1H), 7.75 (d, $J = 7.9$ Hz, 1H), 7.41 (m, 2H), 7.25 (dd, $J = 8.9, 2.5$ Hz, 1H), 7.07 (d, $J = 8.8$ Hz, 1H), 7.00 (d, $J = 2.4$ Hz, 1H), 6.69 (d, $J = 2.7$ Hz, 1H), 6.59 (dd, $J = 8.8, 2.7$ Hz, 1H), 5.99 (d, $J = 5.0$ Hz, 1H), 2.70 (d, $J = 5.0$ Hz, 3H).

3,5-Dichloro-*N*-(3-chloro-4-(naphthalen-2-yloxy)phenyl)-2-hydroxy-*N*-methylbenzamide (**12**). To a stirred solution of 30 mg (0.106 mmol) of **11** in 5 mL of CH_2Cl_2 was added 29 mg (0.127 mmol, 1.2 equiv) of **5a**, and the mixture was left stirring at room temperature for 0.5 h. The reaction was monitored by TLC (CH_2Cl_2), and once completed, routine aqueous workup was performed, and the organic phase was concentrated and purified by column chromatography (CH_2Cl_2) to obtain **9** as a white solid. Yield 48%; $R_f = 0.42$ (CH_2Cl_2); 1H NMR (300 MHz, DMSO- d_6) δ 10.28 (s, 1H), 7.96 (d, $J = 8.9$ Hz, 1H), 7.92 (d, $J = 7.9$ Hz, 1H), 7.76 (d, $J = 8.2$ Hz, 1H), 7.62 (d, $J = 2.4$ Hz, 1H), 7.51 (d, $J = 2.4$ Hz, 1H), 7.48 (dt, $J = 19.9, 6.7$ Hz, 2H), 7.24 (d, $J = 3.3$ Hz, 1H), 7.22 (dd, $J = 11.1, 2.5$ Hz, 1H), 7.20 (d, $J = 1.7$ Hz, 1H), 7.13 (dd, $J = 8.6, 2.4$ Hz, 1H), 7.08 (d, $J = 1.3$ Hz, 1H), 3.35 (s, 3H). MS (ESI): m/z 470.1 $[M - H]^-$.

AUTHOR INFORMATION

Corresponding Author

*Telephone: (520) 626-5957. Fax: (520) 626-8657. E-mail: mjacobson@pharmacy.arizona.edu.

Present Addresses

⁵Elan Pharmaceuticals, 800 Gateway Boulevard, South San Francisco, California 94080, United States.

ACKNOWLEDGMENT

This research was supported in part by NIH Grants CA43894, CA27502, and CA090085 (M.K.J.), a grant from Telik Inc., and a predoctoral fellowship from the ACS Division of Medicinal Chemistry sponsored by Amgen (to J.D.S.). The authors thank Trevigen Inc. for providing PARP-1 and PAR ELISA kits. M.K.J. serves as a consultant to Trevigen.

ABBREVIATIONS USED

ADP, adenosine diphosphate; PAR, poly(ADP-ribose); PARP, poly(ADP-ribose) polymerase; BRCA1/2, breast cancer susceptibility protein 1/2; PARG, poly(ADP-ribose) glycohydrolase; NAD^+ , the oxidized form of nicotinamide adenine dinucleotide; $NAD(H)$, the total cellular pool of nicotinamide adenine dinucleotide, both oxidized and reduced forms; TRAP, target-related affinity profiling; IC_{50} , half maximal inhibitory concentration; HBD, hydrogen bond donor; HBA, hydrogen bond acceptor; SAR, structure–activity relationship; ADP-HPD, adenosine 5'-diphosphate (hydroxymethyl) pyrrolidinediol; MNNG, *N*-methyl-*N'*-nitro-*N*-nitrosoguanidine

REFERENCES

(1) Diefenbach, J.; Burkle, A. Introduction to poly(ADP-ribose) metabolism. *Cell. Mol. Life Sci.* **2005**, *62* (7–8), 721–730.

(2) Juarez-Salinas, H.; Sims, J. L.; Jacobson, M. K. Poly(ADP-ribose) levels in carcinogen-treated cells. *Nature* **1979**, *282* (5740), 740–741.

(3) Hottiger, M. O.; Hassa, P. O.; Luscher, B.; Schuler, H.; Koch-Nolte, F. Toward a unified nomenclature for mammalian ADP-ribosyltransferases. *Trends Biochem. Sci.* **2010**, *35* (4), 208–219.

(4) Davidovic, L.; Vodenicharov, M.; Affar, E. B.; Poirier, G. G. Importance of poly(ADP-ribose) glycohydrolase in the control of poly(ADP-ribose) metabolism. *Exp. Cell Res.* **2001**, *268* (1), 7–13.

(5) Braun, S. A.; Panzeter, P. L.; Collinge, M. A.; Althaus, F. R. Endoglycosidic cleavage of branched polymers by poly(ADP-ribose) glycohydrolase. *Eur. J. Biochem.* **1994**, *220* (2), 369–375.

(6) Alvarez-Gonzalez, R.; Jacobson, M. K. Characterization of polymers of adenosine diphosphate ribose generated in vitro and in vivo. *Biochemistry* **1987**, *26* (11), 3218–3224.

(7) D'Amours, D.; Desnoyers, S.; D'Silva, I.; Poirier, G. G. Poly(ADP-ribosylation) reactions in the regulation of nuclear functions. *Biochem. J.* **1999**, *342* (Part 2), 249–268.

(8) Jacobson, M. K.; Levi, V.; Juarez-Salinas, H.; Barton, R. A.; Jacobson, E. L. Effect of carcinogenic *N*-alkyl-*N*-nitroso compounds on nicotinamide adenine dinucleotide metabolism. *Cancer Res.* **1980**, *40* (6), 1797–1802.

(9) Berger, N. A. Poly(ADP-ribose) in the cellular response to DNA damage. *Radiat. Res.* **1985**, *101* (1), 4–15.

(10) Curtin, N. J. PARP inhibitors for cancer therapy. *Expert Rev. Mol. Med.* **2005**, *7* (4), 1–20.

(11) Ferraris, D. V. Evolution of poly(ADP-ribose) polymerase-1 (PARP-1) inhibitors. From concept to clinic. *J. Med. Chem.* **2010**, *53* (12), 4561–4584.

(12) Rouleau, M.; Patel, A.; Hendzel, M. J.; Kaufmann, S. H.; Poirier, G. G. PARP inhibition: PARP1 and beyond. *Nat. Rev. Cancer* **2010**, *10* (4), 293–301.

(13) Sunderland, P. T.; Dhami, A.; Mahon, M. F.; Jones, L. A.; Tully, S. R.; Lloyd, M. D.; Thompson, A. S.; Javaid, H.; Martin, N. M.; Threadgill, M. D. Synthesis of 4-alkyl-, 4-aryl- and 4-arylamino-5-aminoisoquinolin-1-ones and identification of a new PARP-2 selective inhibitor. *Org. Biomol. Chem.* **2011**, *9* (3), 881–891.

(14) Plummer, E. R. Inhibition of poly(ADP-ribose) polymerase in cancer. *Curr. Opin. Pharmacol.* **2006**, *6* (4), 364–368.

(15) Bryant, H. E.; Schultz, N.; Thomas, H. D.; Parker, K. M.; Flower, D.; Lopez, E.; Kyle, S.; Meuth, M.; Curtin, N. J.; Helleday, T. Specific killing of BRCA2-deficient tumours with inhibitors of poly(ADP-ribose) polymerase. *Nature* **2005**, *434* (7035), 913–917.

(16) Farmer, H.; McCabe, N.; Lord, C. J.; Tutt, A. N.; Johnson, D. A.; Richardson, T. B.; Santarosa, M.; Dillon, K. J.; Hickson, I.; Knights, C.; Martin, N. M.; Jackson, S. P.; Smith, G. C.; Ashworth, A. Targeting the DNA repair defect in BRCA mutant cells as a therapeutic strategy. *Nature* **2005**, *434* (7035), 917–921.

(17) Min, W.; Wang, Z. Q. Poly (ADP-ribose) glycohydrolase (PARG) and its therapeutic potential. *Front. Biosci.* **2009**, *14*, 1619–1626.

(18) Koh, D. W.; Lawler, A. M.; Poitras, M. F.; Sasaki, M.; Wattler, S.; Nehls, M. C.; Stoger, T.; Poirier, G. G.; Dawson, V. L.; Dawson, T. M. Failure to degrade poly(ADP-ribose) causes increased sensitivity to cytotoxicity and early embryonic lethality. *Proc. Natl. Acad. Sci. U.S.A.* **2004**, *101* (51), 17699–17704.

(19) Cortes, U.; Tong, W. M.; Coyle, D. L.; Meyer-Ficca, M. L.; Meyer, R. G.; Petrilli, V.; Herceg, Z.; Jacobson, E. L.; Jacobson, M. K.; Wang, Z. Q. Depletion of the 110-kilodalton isoform of poly(ADP-ribose) glycohydrolase increases sensitivity to genotoxic and endotoxic stress in mice. *Mol. Cell. Biol.* **2004**, *24* (16), 7163–7178.

(20) Gao, H.; Coyle, D. L.; Meyer-Ficca, M. L.; Meyer, R. G.; Jacobson, E. L.; Wang, Z. Q.; Jacobson, M. K. Altered poly(ADP-ribose) metabolism impairs cellular responses to genotoxic stress in a hypomorphic mutant of poly(ADP-ribose) glycohydrolase. *Exp. Cell Res.* **2007**, *313* (5), 984–996.

(21) Blenn, C.; Althaus, F. R.; Malanga, M. Poly(ADP-ribose) glycohydrolase silencing protects against H_2O_2 -induced cell death. *Biochem. J.* **2006**, *396* (3), 419–429.

- (22) Cohausz, O.; Blenn, C.; Malanga, M.; Althaus, F. R. The roles of poly(ADP-ribose)-metabolizing enzymes in alkylation-induced cell death. *Cell. Mol. Life Sci.* **2008**, *65* (4), 644–655.
- (23) Burns, D. M.; Ying, W.; Kauppinen, T. M.; Zhu, K.; Swanson, R. A. Selective down-regulation of nuclear poly(ADP-ribose) glycohydrolase. *PLoS One* **2009**, *4* (3), No. e4896.
- (24) Tang, J. B.; Svilar, D.; Trivedi, R. N.; Wang, X. H.; Goellner, E. M.; Moore, B.; Hamilton, R. L.; Banze, L. A.; Brown, A. R.; Sobol, R. W. N-Methylpurine DNA glycosylase and DNA polymerase {beta} modulate BER inhibitor potentiation of glioma cells to temozolomide. *Neuro-Oncology* **2011**, *13* (5), 471–486.
- (25) Tanuma, S.; Sakagami, H.; Endo, H. Inhibitory effect of tannin on poly(ADP-ribose) glycohydrolase from human placenta. *Biochem. Int.* **1989**, *18* (4), 701–708.
- (26) Bakondi, E.; Bai, P.; Erdelyi, K.; Szabo, C.; Gergely, P.; Virag, L. Cytoprotective effect of gallotannin in oxidatively stressed HaCaT keratinocytes: the role of poly(ADP-ribose) metabolism. *Exp. Dermatol.* **2004**, *13* (3), 170–178.
- (27) Ying, W.; Sevigny, M. B.; Chen, Y.; Swanson, R. A. Poly(ADP-ribose) glycohydrolase mediates oxidative and excitotoxic neuronal death. *Proc. Natl. Acad. Sci. U.S.A.* **2001**, *98* (21), 12227–12232.
- (28) Tavassoli, M.; Tavassoli, M. H.; Shall, S. Effect of DNA intercalators on poly(ADP-ribose) glycohydrolase activity. *Biochim. Biophys. Acta* **1985**, *827* (3), 228–234.
- (29) Ramsinghani, S.; Koh, D. W.; Ame, J. C.; Strohm, M.; Jacobson, M. K.; Slama, J. T. Syntheses of photoactive analogues of adenosine diphosphate (hydroxymethyl)pyrrolidinediol and photoaffinity labeling of poly(ADP-ribose) glycohydrolase. *Biochemistry* **1998**, *37* (21), 7801–7812.
- (30) Slama, J. T.; Aboul-Ela, N.; Goli, D. M.; Cheesman, B. V.; Simmons, A. M.; Jacobson, M. K. Specific inhibition of poly(ADP-ribose) glycohydrolase by adenosine diphosphate (hydroxymethyl)pyrrolidinediol. *J. Med. Chem.* **1995**, *38* (2), 389–393.
- (31) Slama, J. T.; Aboul-Ela, N.; Jacobson, M. K. Mechanism of inhibition of poly(ADP-ribose) glycohydrolase by adenosine diphosphate (hydroxymethyl)pyrrolidinediol. *J. Med. Chem.* **1995**, *38* (21), 4332–4336.
- (32) Li, J.; Ferraris, D.; Kletzly, P.; Li, W.; Wang, E.; Xing, A.; Xu, W.; Zhang, J. Symmetrically Disubstituted Aromatic Compounds and Pharmaceutical Compositions for Inhibiting Poly(ADP-ribose) Glycohydrolase, And Methods for Their Use. WO 02057211, 2002.
- (33) Falsig, J.; Christiansen, S. H.; Feuerhahn, S.; Burkde, A.; Oei, S. L.; Keil, C.; Leist, M. Poly(ADP-ribose) glycohydrolase as a target for neuroprotective intervention: assessment of currently available pharmacological tools. *Eur. J. Pharmacol.* **2004**, *497* (1), 7–16.
- (34) Labieniec, M.; Gabryelak, T.; Falcioni, G. Antioxidant and pro-oxidant effects of tannins in digestive cells of the freshwater mussel *Unio tumidus*. *Mutat. Res.* **2003**, *539* (1–2), 19–28.
- (35) Blenn, C.; Wyrsh, P.; Althaus, F. R. The ups and downs of tannins as inhibitors of poly(ADP-ribose)glycohydrolase. *Molecules* **2011**, *16* (2), 1854–1877.
- (36) Beroza, P.; Damodaran, K.; Lum, R. T. Target-related affinity profiling: Telik's lead discovery technology. *Curr. Top. Med. Chem.* **2005**, *5* (4), 371–381.
- (37) Suezawa, H.; Hirota, M.; Yuzuri, T.; Hamada, Y.; Takeuchi, I.; Sugiura, M. Studies on the conformations of antimicrobial salicylanilide derivatives by spectroscopy. *Bull. Chem. Soc. Jpn.* **2000**, *73*, 2335–2339.
- (38) Botta, D.; Jacobson, M. K. Identification of a regulatory segment of poly(ADP-ribose) glycohydrolase. *Biochemistry* **2010**, *49* (35), 7674–7682.
- (39) Rankin, P. W.; Jacobson, E. L.; Benjamin, R. C.; Moss, J.; Jacobson, M. K. Quantitative studies of inhibitors of ADP-ribosylation in vitro and in vivo. *J. Biol. Chem.* **1989**, *264* (8), 4312–4317.
- (40) Hassa, P. O.; Hottiger, M. O. The diverse biological roles of mammalian PARPs, a small but powerful family of poly-ADP-ribose polymerases. *Front. Biosci.* **2008**, *13*, 3046–3082.
- (41) Berger, N. A.; Berger, S. J. Metabolic consequences of DNA damage: the role of poly (ADP-ribose) polymerase as mediator of the suicide response. *Basic Life Sci.* **1986**, *38*, 357–363.
- (42) Andrabi, S. A.; Kim, N. S.; Yu, S. W.; Wang, H.; Koh, D. W.; Sasaki, M.; Klaus, J. A.; Otsuka, T.; Zhang, Z.; Koehler, R. C.; Hurn, P. D.; Poirier, G. G.; Dawson, V. L.; Dawson, T. M. Poly(ADP-ribose) (PAR) polymer is a death signal. *Proc. Natl. Acad. Sci. U.S.A.* **2006**, *103* (48), 18308–18313.
- (43) Virag, L.; Szabo, C. The therapeutic potential of poly(ADP-ribose) polymerase inhibitors. *Pharmacol. Rev.* **2002**, *54* (3), 375–429.
- (44) Szabo, C. Pharmacological inhibition of poly(ADP-ribose) polymerase in cardiovascular disorders: future directions. *Curr. Vasc. Pharmacol.* **2005**, *3* (3), 301–303.
- (45) Sodhi, R. K.; Singh, N.; Jaggi, A. S. Poly(ADP-ribose) polymerase-1 (PARP-1) and its therapeutic implications. *Vasc. Pharmacol.* **2010**, *53* (3–4), 77–87.
- (46) Genovese, T.; Di Paola, R.; Catalano, P.; Li, J. H.; Xu, W.; Massuda, E.; Caputi, A. P.; Zhang, J.; Cuzzocrea, S. Treatment with a novel poly(ADP-ribose) glycohydrolase inhibitor reduces development of septic shock-like syndrome induced by zymosan in mice. *Crit. Care Med.* **2004**, *32* (6), 1365–1374.
- (47) Lu, X. C.; Massuda, E.; Lin, Q.; Li, W.; Li, J. H.; Zhang, J. Post-treatment with a novel PARG inhibitor reduces infarct in cerebral ischemia in the rat. *Brain Res.* **2003**, *978* (1–2), 99–103.
- (48) Lin, W.; Ame, J. C.; Aboul-Ela, N.; Jacobson, E. L.; Jacobson, M. K. Isolation and characterization of the cDNA encoding bovine poly(ADP-ribose) glycohydrolase. *J. Biol. Chem.* **1997**, *272* (18), 11895–11901.
- (49) Menard, L.; Poirier, G. G. Rapid assay of poly(ADP-ribose) glycohydrolase. *Biochem. Cell Biol.* **1987**, *65* (7), 668–673.
- (50) Jacobson, E. L.; Jacobson, M. K. Pyridine nucleotide levels as a function of growth in normal and transformed 3T3 cells. *Arch. Biochem. Biophys.* **1976**, *175* (2), 627–634.